The Structure of 1-Chlorosilatrane: An *Ab Initio* Molecular Orbital and a Density Functional Theory Study

GÁBOR I. CSONKA* and PÁL HENCSEI

Department of Inorganic Chemistry, Technical University of Budapest, H-1521 Budapest, Hungary

Received 7 November 1994; accepted 2 June 1995

ABSTRACT

The molecular geometries of the 1-chloro-, 1-fluoro-, 1-methyl-, and 1-hydrogenosilatranes were fully optimized by the restricted Hartree-Fock (HF) method supplemented with 3-21G, 3-21G(*d*), 6-31G(*d*), and CEP-31G(*d*) basis sets; by MP2 calculations using 6-31G(*d*) and CEP-31G(*d*) basis sets; and by GGA-DFT calculations using 6-31G(*d*5) basis set with the aim of locating the positions of the local minima on the energy hypersurface. The HF/6-31G(*d*) calculations predict long (> 254 pm) and the MP2/CEP calculations predicted short (~ 225 pm) equilibrium Si—N distances. The present GGA-DFT calculations reproduce the available gas phase experimental Si—N distances correctly. The solid phase experimental results predict that the Si—N distance is shorter in 1-chlorosilatrane than in 1-fluorosilatrane. In this respect the HF results show a strong basis set dependence, the MP2/CEP results contradict the experiment, and the GGA-DFT results in electrolytic medium agree with the experiment. The latter calculations predict that 1-chlorosilatrane is more polarizable than 1-fluorosilatrane and also support a general Si—N distance shortening trend for silatranes during the transition from gas phase to polar liquid or solid phase. The calculations predict that the ethoxy links of the silatrane skeleton are flexible. Consequently, it is difficult to measure experimentally the related bond lengths and bond and torsion angles. This is the probable origin of the surprisingly large differences for the experimental structural parameters. On the basis of experimental analogies, *ab initio* calculations, and density functional theory (DFT) calculations, a gas phase equilibrium (r_e) geometry is predicted for 1-chlorosilatrane. The semiempirical methods predict a so-called exo minimum (at above 310 pm Si—N distance); however, the *ab initio* and GGA-DFT calculations suggest that this form is nonexistent. The GGA-DFT geometry optima were characterized by frequency analysis.

*Author to whom all correspondence should be addressed.

Journal of Computational Chemistry, Vol. 17, No. 7, 767–780 (1996)

CCC 0192-8651 / 96 / 070767-14

Introduction

This study is the continuation of our previous studies, which have reported the MNDO, AM1, and PM3 equilibrium conformations of 1-fluoro-, 1-methyl-, and 1-chlorosilatrane[1-3] and *ab initio* Hartree-Fock (HF) equilibrium conformations of 1-fluorosilatrane.[4] Silatranes—the $RSi(OCH_2CH_2)_3N$, 1-organyl-2,8,9-trioxa-5-aza-1-silatricyclo [3.3.3.0^{1,5}] undecanes—are biologically active, neutral hypervalent compounds.[5] The transannular Si—N donor–acceptor bond (Figs. 1 and 2) makes these molecules especially interesting and challenging for theoretical and experimental studies.

Short Si—N distances (202–225 pm) were observed in X-ray experiments of many substituted silatranes. Gas phase electron diffraction (ED) measurements, however, gave longer Si—N distances in 1-fluorosilatrane[6,7] and in 1-methylsilatrane.[8,9] In 1-chlorosilatrane the Si—N distance is 202.3 pm (X-ray),[10] which is the shortest Si—N distance measured, while no ED data are available. All measured Si—N distances are longer than the sum of the covalent radii (~ 175 pm) but shorter than the sum of the appropriate nonbonded radii (269 pm)[11] and much shorter than the sum of van der Waals radii (350 pm). The Si—N distance is also variable in solution, shortening in polar solvents and lengthening in nonpolar solvents.[12] The Si—N distance has also been found to be dependent on the nature of substituent R at silicon. An electron withdrawing substituent shortens the experimental Si—N distance. Methyl substitution lengthens the Si—N distance by about 13 pm.

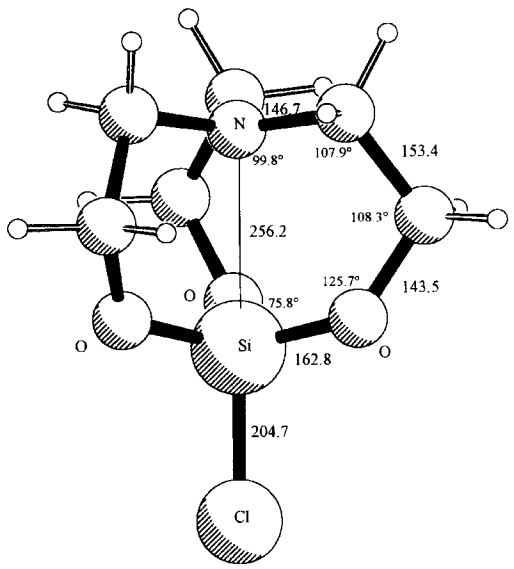

FIGURE 1. The molecular diagram of HF / 6-31G(*d*) equilibrium geometry of 1-chlorosilatrane. The bond distances are in pm and the bond angles are in degrees.

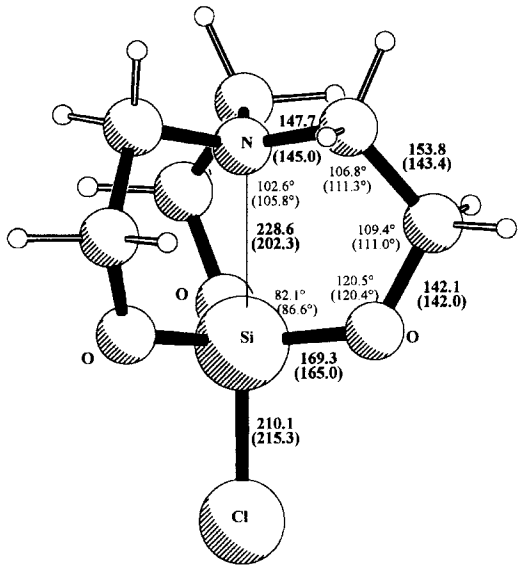

FIGURE 2. The molecular diagram of B-P / 6-31G(*d*5) equilibrium geometry of 1-chlorosilatrane. The bond distances are in pm and the bond angles are in degrees. A fine grid was used to calculate the DFT integrals. The experimental (X-ray) values are in parentheses.

Our recent articles[1-4] discuss the reliability of semiempirical and HF methods for silatranes. The earlier theoretical results are extensively discussed in those articles, and we do not intend to repeat here the literature overview. The interested reader should refer to ref. 4. It was found that the semiempirical potential energy curve follows closely the HF potential energy curve in the vicinity of the energy minimum (endo form); however, considerable differences occur at larger Si—N distances (above 290 pm, exo form).[4] The exo form was never found in experiments, and the HF results show that it may not exist. The HF and semiempirical results agree with each other in that the silatrane skeleton is flexible, and low-energy, large-amplitude motions occur in silatranes. Various experimental discrepancies and the large differences between the X-ray and ED Si—N distances can be explained by these facts.[4]

In this article the *ab initio* and DFT results for several silatranes are summarized. We analyze first the X-ray and ED experimental results. Next we

provide the HF potential energy curve (PEC) for the Si—N distance and the structural changes of the silatrane skeleton as a function of Si—N distance in 1-chlorosilatrane. We give the HF, MP2, and generalized gradient approximation density functional theory (GGA-DFT) equilibrium geometries for silatranes and predict a probable gas phase structure for the 1-chlorosilatrane. Next we give the results of the medium effects on the ring conformations. We also give the correlated PEC for large Si—N distances and the results of the GGA-DFT frequency analysis for the equilibrium geometries.

Computational Methods

The geometries of silatranes were optimized with HF, many-body perturbation theory (MBPT) using Møller-Plesset partition to the second order (MP2)[13] and GGA-DFT methods. C_3 symmetry of the silatrane skeleton was conserved during the geometry optimizations. For the PEC studies, the Si—N distance was fixed and all the other geometric parameters were relaxed.

For the GGA-DFT methods, the combinations of the functionals were as follows:

1. The **B-P** or Becke-Perdew method was used, in which Becke's GGA exchange functional[14] is combined with Perdew's GGA correlation functional.[15]
2. The **B3-P** method is a hybrid. It is a linear combination of various exchange and correlational functionals in the form

$$A \cdot E_x[\mathrm{HF}] + (1 - A) \cdot E_x[\mathrm{S}] + B \cdot \Delta E_x[\mathrm{B}] + E_c[\mathrm{VWN}] + C \cdot \Delta E_c[\mathrm{P86}]$$

where E_x[HF], E_x[S], and E_x[B] are the Slater, HF, and Becke[14] exchange functionals and E_c[VWN] and ΔE_c[P86] are the Vosko, Wilk, and Nussair[16] and Perdew[15] correlation functionals, respectively. Note that ΔE_x[B] is a gradient correction to the S + WVN or LSDA, for exchange, and ΔE_c[P86] is a gradient correction for correlation. The constants A, B, and C are those determined by Becke by fitting heats of formation ($A = 0.2$, $B = 0.72$, $C = 0.81$).[17] Note that Becke used the Perdew-Wang (PW91) functional instead of P86.

GAUSSIAN 92/DFT[18] uses numerical quadrature to evaluate the DFT integrals. The quadrature scheme is defined by the number of points in radial and angular directions. The geometries were optimized first with a normal grid (50 radial shells, 194 angular points per shell, and pruned to about 3000 points per atom). Next we reoptimized the geometries with a finer grid (75 radial shells, 302 angular points per shell, and pruned to about 7000 points per atom). The latter has considerably better numerical accuracy and rotational invariance properties than the normal grid. The HF and DFT minima were checked by frequency analysis.

GGA-DFT calculations were carried out using the 6-31G(d5) basis set supplemented with five d functions. HF calculations were carried out using compact effective potential plus single or double polarization CEP-31(d) basis sets[19] and split-valence plus single polarization 3-21G, 3-21G(d), and 6-31G(d) basis sets (single-zeta core, double-zeta valence and polarization functions)[20] supplemented with six d functions. MP2 frozen core (MP2 = FC) calculations were carried out using CEP-31(d) and 6-31G(d) basis sets. The CEP-31G(d) basis set is computationally advantageous for 1-chlorosilatrane.

The calculations were carried out using Silicon Graphics workstations.

Problems with Experimental Geometries: Analysis of Crystallographic Data

The key structural parameter of silatranes is the Si—N distance. The experimental results and the quantum chemical calculations show that this distance is sensitive to the nature of the substituent on the silicon atom (Table I). The various substituted silatranes can be put into an order on the basis of this distance. The shortest Si—N distance known in solid phase was measured in 1-chlorosilatrane.[10] This fact is surprising at first sight, because on the basis of the electronegativities of halogen atoms, a shorter Si—N distance is expected in 1-fluorosilatrane than in 1-chlorosilatrane. One possible explanation for the opposite experimental results is that the N—Si—X (where X is the substituent on the Si atom) interaction in silatranes may be better modeled by an intramolecular S_N2 reaction, in which the N is approaching the Si and the group on the opposite side is leaving. The chlorine is a better leaving

TABLE I.
Equilibrium Geometrical Parameters for Silatranes.[a]

Substituent	Cl	F	Me	H
Bond length (Si—N) AM1	257.9	253.2	260.3	
PM3	245.5	250.2	256.3	
HF / 3-21G	222.8	239.7	263.7	
HF / 3-21G(*d*)	256.3	258.5	275.1	266.5
HF / 6-31G(*d*)	257.3	255.6	274.5	265.7
HF / CEP-31G(*d*)	253.5	245.6		263.4
MP2 / 6-31G(*d*)				231.4
MP2 / CEP-31G(*d*)	226.2	224.1		231.2
B3-P / 6-31G(*d*5)	230.5	231.7	247.3	233.9
B3-P / 6-31G(*d*5)[b]		228.4		
B-P / 6-31G(*d*5)	230.8	233.1	244.8	232.2
B-P / 6-31G(*d*5)[b]	228.6	230.2		231.6
ED (r_g)	—	232.4 ± 1.4	245.3(47)	
X-ray (esd)	202.3	204.2(1)	217.5(4)	
Bond length (Si—R) AM1	205.8	160.0	178.7	
PM3	210.6	158.8	190.5	
HF / 3-21G	217.0	161.5	187.0	
HF / 3-21G(*d*)	204.6	158.1	185.5	146.0
HF / 6-31G(*d*)	205.8	158.1	186.1	145.9
HF / CEP-31G(*d*)	207.7	159.4		147.1
MP2 / 6-31G(*d*)				147.6
MP2 / CEP-31G(*d*)	209.4	163.5		148.7
B3-P / 6-31G(*d*5)	207.8	160.7	186.3	147.4
B-P / 6-31G(*d*5)	210.0	162.3	188.1	148.8
ED (r_g)	—	156.8 ± 0.6	185.3(15)	
X-ray (esd)	215.3	162.2(1)	187.0(6)	
Bond length (Si—O) AM1	176.6	176.2	177.4	
PM3	170.4	170.9	171.3	
HF / 3-21G	166.5	165.7	166.8	
HF / 3-21G(*d*)	162.8	162.7	163.9	163.7
HF / 6-31G(*d*)	163.3	163.6	164.6	164.4
HF / CEP-31G(*d*)	164.1	164.3		165.2
MP2 / 6-31G(*d*)				169.1
MP2 / CEP-31G(*d*)	169.1	169.0		170.3
B3-P / 6-31G(*d*5)	166.9	166.7	167.8	168.1
B-P / 6-31G(*d*5)	169.1	168.8	170.1	170.3
ED (r_g)	—	165.2 ± 0.3	165.6	
X-ray (esd)	164.4	163.8(2)	165.7(3)	
	165.1	164.3(2)	167.3(4)	
	165.2	165.4(2)	168.0(4)	
Bond length (C—N) AM1	144.8	144.9	144.6	
PM3	148.6	148.4	148.1	
HF / 3-21G	148.6	147.8	146.5	
HF / 3-21G(*d*)	146.7	146.7	145.9	146.3
HF / 6-31G(*d*)	144.9	145.0	144.3	144.6
HF / CEP-31G(*d*)	146.0	146.3		145.7
MP2 / 6-31G(*d*)				146.5
MP2 / CEP-31G(*d*)	148.3	148.4		148.0
B3-P / 6-31G(*d*5)	146.2	146.2	145.3	145.9
B-P / 6-31G(*d*5)	147.8	147.6	146.9	147.5
ED (r_g)	—	148.1 ± 0.8	145.8(6)	
X-ray (esd)	144.2	145.4(7), 145.5(8)	147.3(6)	
	145.2	146.5(5), 145.4(6)	147.3(6)	
	145.4	149.0(3), 147.1(6)	148.8(6)	

[a]Bond lengths are in pm, bond angles are in degrees. The experimental values are from refs. 6–10. The AM1 and PM3 values are from refs. 1–3. The HF / 3-21G, 3-21G(*d*), and 6-31G(*d*) values for 1-fluorosilatrane are from ref. 4.
[b]DFT results calculated with a fine grid.

(Continues on next page)

TABLE I.
(continued)

Substituent	Cl	F	Me	H
Bond length (C—C) AM1	154.8	154.9	154.7	
PM3	154.5	154.8	154.3	
HF / 3-21G	153.8	153.6	153.7	
HF / 3-21G(*d*)	153.4	153.5	153.5	153.5
HF / 6-31G(*d*)	152.7	152.8	152.8	152.8
HF / CEP-31G(*d*)	154.0	154.0		154.0
MP2 / 6-31G(*d*)				152.5
MP2 / CEP-31G(*d*)	154.4	154.5		154.6
B3-P / 6-31G(*d*5)	152.6	152.7	152.8	152.7
B-P / 6-31G(*d*5)	153.8	154.0	154.8	154.1
ED (r_g)	—	151.4 ± 1.1	155.8(10)	
X-ray (esd)	142.7	146.1(6), 153.0(3)	151.4(8)	
	143.3	148.0(6), 148.7(7)	153.0(8)	
	144.3	145.0(7), 152.9(6)	153.4(8)	
Bond length (C—O) AM1	138.8	138.8	138.7	
PM3	138.6	138.6	138.5	
HF / 3-21G	142.3	142.2	142.2	
HF / 3-21G(*d*)	143.5	143.4	143.4	143.1
HF / 6-31G(*d*)	140.1	139.8	140.1	139.8
HF / CEP-31G(*d*)	141.0	140.5		140.8
MP2 / 6-31G(*d*)				141.5
MP2 / CEP-31G(*d*)	143.1	142.8		142.8
B3-P / 6-31G(*d*5)	140.4	140.1	140.1	140.0
B-P / 6-31G(*d*5)	142.1	141.7	141.6	141.5
ED (r_g)	—	139.2 ± 0.4	141.4(5)	
X-ray (esd)	140.8	140.8(2)	141.8(6)	
	141.9	140.9(4)	142.7(7)	
	142.1	141.4(4)	142.9(7)	
Bond angle (O—C—C) AM1	112.3	113.1	113.3	
PM3	113.3	112.7	113.7	
HF / 3-21G	107.6	107.6	109.3	
HF / 3-21G(*d*)	108.3	108.8	109.2	109.0
HF / 6-31G(*d*)	109.8	109.7	110.7	110.4
HF / CEP-31G(*d*)	109.6	109.4		110.2
MP2 / 6-31G(*d*)				108.9
MP2 / CEP-31G(*d*)	108.3	108.4		108.8
B3-P / 6-31G(*d*5)	109.2	109.1	110.0	109.7
B-P / 6-31G(*d*5)	109.4	109.4	110.2	110.0
ED (r_g)	—	117.0 ± 0.7	116.4(16)	
X-ray (esd)	110.3	110.7(5), 109.9(5)	107.7(7)	
	111.4	111.1(5), 111.4(6)	108.5(7)	
	111.6	111.1(5), 109.4(5)	109.9(6)	
Bond angle (N—C—C) AM1	110.1	110.4	110.2	
PM3	107.6	108.0	107.4	
HF / 3-21G	106.4	106.8	108.3	
HF / 3-21G(*d*)	107.9	108.9	109.3	108.6
HF / 6-31G(*d*)	108.8	108.7	110.3	109.5
HF / CEP-31G(*d*)	108.0	107.6		108.7
MP2 / 6-31G(*d*)				106.4
MP2 / CEP-31G(*d*)	105.6	105.7		106.0
B3-P / 6-31G(*d*5)	106.9	106.9	107.7	107.3
B-P / 6-31G(*d*5)	106.8	106.9	107.5	107.1
ED (r_g)		104.5 ± 0.6	106.7(16)	
X-ray (esd)	110.9	107.8(7), 104.7(6)	104.2(6)	
	111.4	106.7(6), 106.3(7)	105.3(6)	
	112.6	108.0(6), 104.9(6)	106.1(7)	

group than the fluorine, and this may explain the shorter Si—N distance in the case of 1-chlorosilatrane. Unfortunately, no ED measurements are available for 1-chlorosilatrane, so it is not possible to check experimentally whether the shorter Si—N distance also appears in the gas phase. The available solid and gaseous state structures for 1-methylsilatrane show that the Si—N distance is considerably (17 pm) larger in 1-methylsilatrane than in 1-fluorosilatrane, independent of the measuring method, as is expected.[8,9]

While the changes of the Si—N distance can be more or less rationalized on the basis of the nature of the group connected to the silicon atom, the X-ray and ED experiments gave surprisingly large variations for the C—N and C—C bond lengths for 1-chloro-, 1-fluoro-, and 1-methylsilatranes. It was noticed in the X-ray experiment for 1-fluorosilatrane that the carbon atoms linked to nitrogen were disordered.[6] As a consequence, the experiment gave six different C—N and C—C bond lengths and O—C—C and N—C—C bond angles (Table I). The existence of different geometries can be attributed to the low-energy intramolecular movements of the ethoxy links and the freezing of different conformations in the solid phase. The X-ray C—C single-bond distances are surprisingly short (143–145 pm) in 1-chloro-[10] and 1-fluorosilatranes[6] while they are normal (153 pm) in 1-methylsilatrane.[8] It is interesting to note that if the experimental C—C bond length is short, the neighboring C—N bond is also short, and if the C—C is long, the C—N bond is long. In the gas phase ED geometries, the situation is different. If the measured C—N distance is long, then the C—C distance is short (in 1-fluorosilatrane),[7] or if the C—N distance is short, then the C—C distance is long (in 1-methylsilatrane).[9] It seems that the sum of the C—N and C—C bond lengths is nearly constant for the ED experiment. The experimental values for bond angles of the silatrane skeleton are also affected by the intramolecular movements. The values for the N—C—C bond angle vary between 104° and 113°. The largest N—C—C bond angle (113°) was found in X-ray structure for 1-chlorosilatrane.[10] The O—C—C bond angles are surprisingly large in the ED experiments (117.0 ± 0.7 and 116.4°),[7,9] which disagrees with the solid phase X-ray and *ab initio* results (between 108 and 111°).[4,6,8,10]

The large experimental differences in the aforementioned structural parameters provided motivation for analyzing several other crystal structures —namely, the relevant structural parameters of the 1-phenyl-,[21] 1-ethyl-,[22] 1-chloromethyl-,[23] and 3-furylsilatranes[24] and the 1-methyl-[25] and 1-phenylsilatranones.[26] Figure 3 shows the experimental C—N and C—C bond lengths, respectively, as a function of Si—N distance. The 1-phenylsilatrane has three and the 1-phenylsilatranone has two different X-ray structures. There are 14 experimental points on the figures in the following order: X = Cl, F, Ph(CO), furyl, chloromethyl, Ph(CO), Ph(γ), Me(CO), Ph(β), Me, Ph(α), Et, F(ED), Me(ED), where (CO) denotes silatranones, (α), (β), and (γ) denote the three different experimental geometries for phenylsilatrane, and (ED) denotes ED results. All other results are from X-ray experiments. The corresponding geometry change curves calculated at the HF level using 3-21G(d) and 6-31G(d) basis sets are also shown in the same figures with solid lines. Those curves are derived from the PEC study and will be discussed in the next section. Figure 4 shows the N—C—C and O—C—C bond angles versus the Si—N distance for the same selected silatranes. Comparison of Figures 3 and 4 shows that the worst agreements between experiment and theory have been found in X-ray structures for the 1-fluoro-,[6] 1-chloro-,[10] and 1-ethyl-substituted[22] silatranes. The X-ray N—C and C—C bond lengths and the N—C—C bond angle in 1-fluorosilatrane[6] show somewhat better agreement with the calculated results than in 1-chlorosilatrane.[10] This slightly better agreement in the former case may be attributed to the correction of the experiment for the disordered carbon atoms. For other molecules the X-ray and ED geometrical parameters and the theory show reasonable agreement. The noticeable exceptions are the previously mentioned large O—C—C bond angles for the two ED structures in Figure 4. There is also a considerable difference between the ED and the calculated O—Si—N—C and C—O—Si—N dihedral angles. The theory supports the X-ray results in this respect. The ED measurements give internuclear distances averaged over a statistical ensemble of vibrational and rotational states. To extract the equilibrium geometries from experimental data, it is necessary to know the large-amplitude anharmonic internal movements and their effects on the measured geometric parameters, which was not known at the time of the aforementioned ED experiments.

These results show that the experimental geometries frequently contradict each other and the theoretical predictions. The probable origin of these contradictions is the large-amplitude low-energy

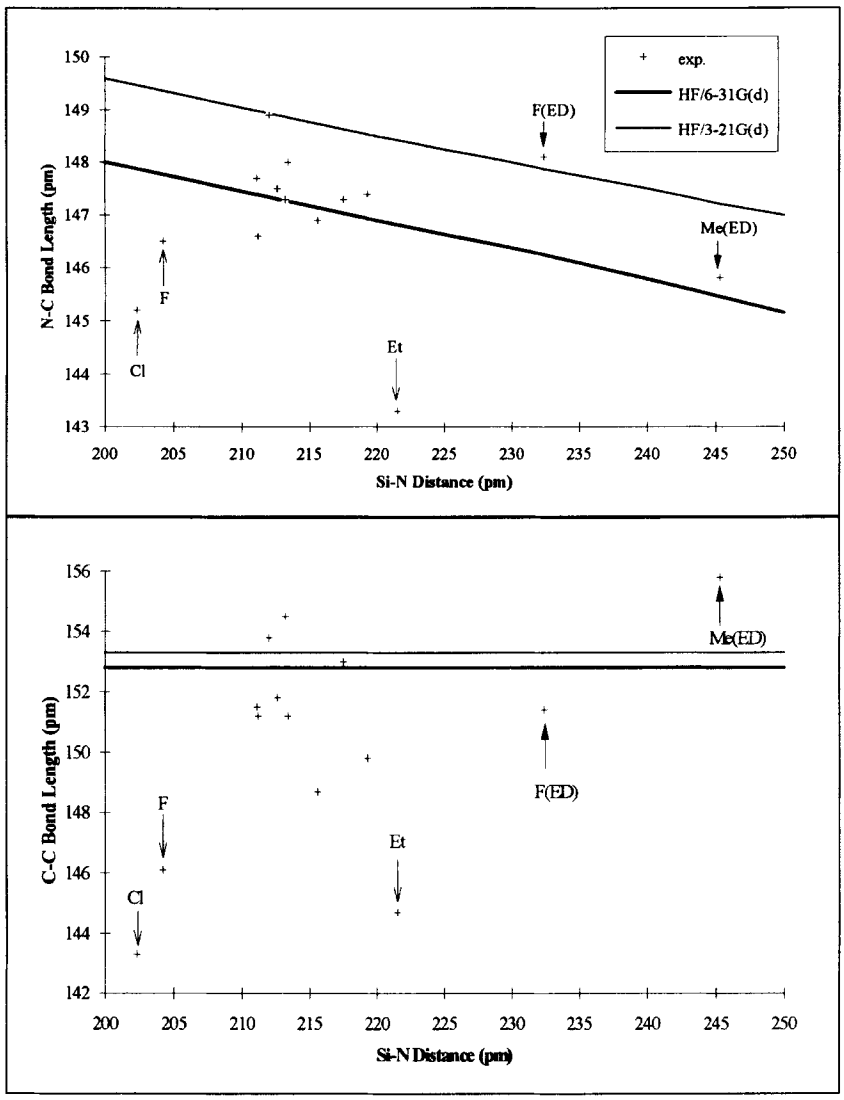

FIGURE 3. Experimental and HF bond lengths versus Si—N distance in various anellated organo-silicon compounds. The experimental results for 1-fluoro-, 1-chloro-, and 1-ethylsilatrane are denoted by arrows. The gas phase results are notated by ED.

movements of the carbon atoms of the ethoxy links and the presence of the two enantiomer structures.

Ab Initio Potential Energy Curves and Structural Changes

Earlier theoretical and experimental studies showed that a small amount of energy is required to shorten or lengthen the Si—N distance from the equilibrium position. The two polarized basis sets at the HF level of theory provided nearly identical results in this respect for 1-chlorosilatrane: Less than 0.02 kcal/mol energy is required to change the Si—N distance around the minimum by ± 3 pm, and 1 kcal/mol energy is sufficient to change the Si—N distance by ± 25 pm.

The structural changes of the silatrane skeleton caused by the large Si—N distance changes are given next. In the S_N2 reaction model, it is expected that as the N gets closer to the silicon atom, the Si—O and Si—Cl bond lengths increase. There is a considerable variation in the Si—Cl bond distance, because the chlorine atom is on the three-center bond axis and it is a good leaving group.

It is expected that the X-ray experiment provides longer C—N distances than the gas phase

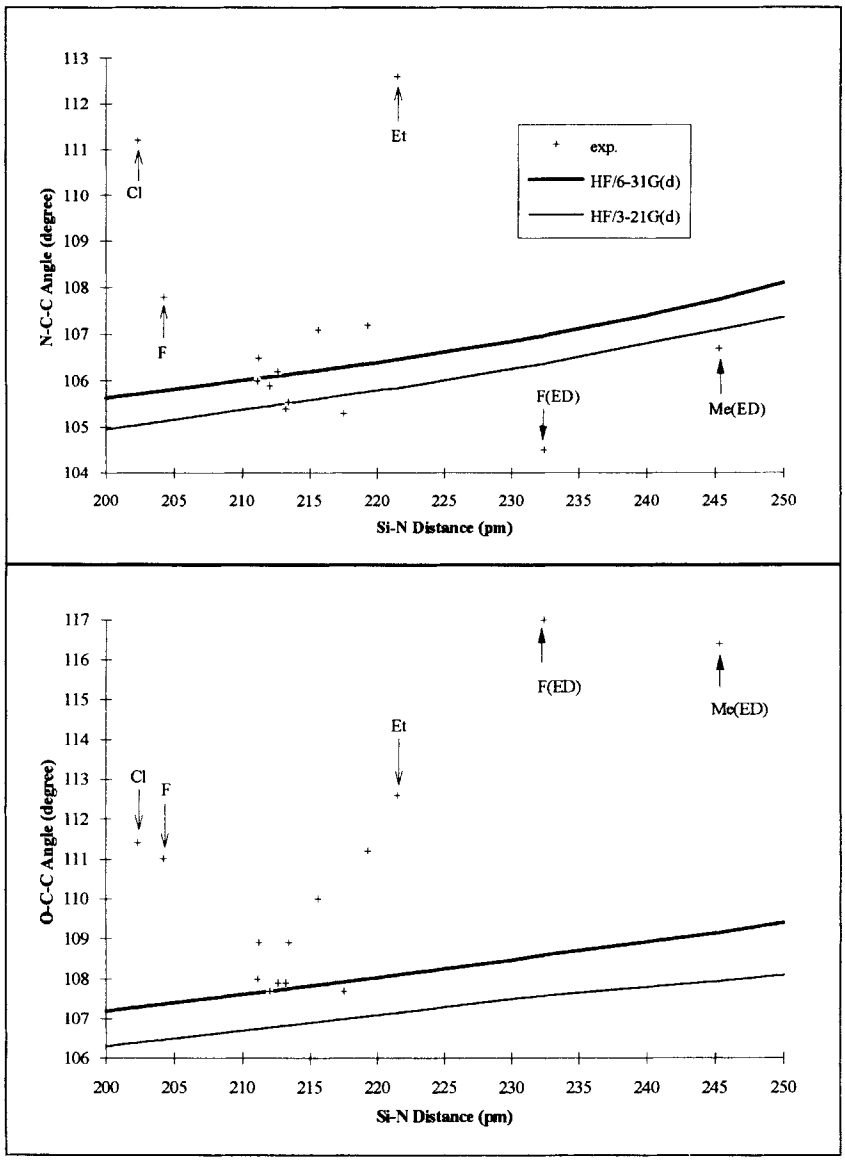

FIGURE 4. Experimental and HF bond angles versus Si—N distance in various anellated organo-silicon compounds. The experimental results for 1-fluoro-, 1-chloro-, and 1-ethylsilatrane are denoted by arrows. The gas phase results are notated by ED.

ED because of the shorter Si—N distance in the former (Fig. 3). This is true for 1-methylsilatrane but not for 1-fluoro- and chlorosilatrane, for which X-ray C—N bond distances are short. The origin of the C—N and C—C bond shortening could be the presence of two enantiomers and of disordered carbon atoms, causing a virtual bond shortening in the X-ray experiment (Fig. 3).

The silatrane skeleton consists of three five-membered rings linked to each other by two anellation atoms (Si and N). We suggest a simple notation for the envelope conformations of the five-membered rings: In the $\mathbf{OC}_0$ envelope the O—Si—N—C dihedral angle is zero. In the $\mathbf{CN}_0$ envelope the C—O—Si—N dihedral angle is zero (see ref. 6). The transition between the two envelope conformations consists of a series of twisted conformations, in which both dihedral angles are negative according to the convention used throughout this article. For the X-ray structure of

1-chlorosilatrane, these dihedral angles are not given explicitly in the original article; consequently, we calculated them from the published crystal coordinates after correcting the misprinted y coordinate of the C_3 atom in ref. 10. The X-ray values for the C—O—Si—N and O—Si—N—C angles vary from $-3.8°$ to $-4.3°$ and from $-8.7°$ to $-9.7°$, respectively. This is a nearly planar twisted conformation, which is different from the $\mathbf{CN}_0$ envelope conformation found by the experiment for 1-fluorosilatrane (C—O—Si—N $\cong -3°$ and O—Si—N—C $\cong -21°$) or the twisted conformations found for 1-methylsilatrane (C—O—Si—N $\cong -8°$ and O—Si—N—C $\cong -17°$). In HF/6-31G(d) optimized geometry, the C—O—Si—N angles are $-30.1°$ and the O—Si—N—C angles are $-0.3°$ ($\mathbf{OC}_0$ envelope conformation). However, at shorter Si—N distances the steric interaction of the electron density of the Si—O and N—C bonds may become important and the O—Si—N—C dihedral would have to open up. If the O—Si—N—C angle is rotated toward the $\mathbf{CN}_0$ envelope conformation, the Si—N and C—O bonds would turn toward an eclipsed position and the oxygen lone pairs would turn away from neighboring Si—F and Si—O bonds. The opposite rotation of the O—Si—N—C angle would force the oxygen lone pairs closer to an eclipsed position with the Si—F and Si—O bonds; clearly, this would not be the preferred position. The consequences for the potential energy curve are discussed in ref. 4.

The calculations show that at the 200 pm Si—N distance, the $\mathbf{CN}_0$ envelope is the most stable conformation. The HF and GGA-DFT results agree well with the X-ray results for C—O—Si—N and O—Si—N—C dihedral angles in 1-fluorosilatrane and 1-methylsilatrane and disagree with the X-ray results for 1-chlorosilatrane. The X-ray structure for 1-chlorosilatrane provides unrealistic flat rings. The ED results for 1-fluorosilatrane[7] [C—O—Si—N $= -2.8(10)°$ and O—Si—N—C $= 20.7(8)°$ at the 232.4 pm Si—N distance] disagree with the calculated values. From the HF and GGA-DFT results we obtain $-19°$ and $-9°$ for the C—O—Si—N and O—Si—N—C angles, respectively, at the 232 pm Si—N distance.

The *ab initio* results also show that the methylene groups of the ethoxy links may jump to the other side of the ring planes (through a planar transition state) and distort the symmetry. The HF/3-21G(d) barrier is only 3 kcal/mol for the $\mathbf{OC}_0$ envelope.

Ab Initio and DFT Equilibrium Geometries

The accuracy of molecular geometries predicted by the HF *ab initio* calculations is extensively discussed in the literature.[27] In HF calculations the electron–electron repulsion terms are underestimated, and the electrons tend to move too close to each other. The stronger Coulombic attraction between electrons and nuclei results in compact covalent bonds. Earlier studies show a general inverse relationship between the quality of the basis set and the predicted covalent bond lengths.[27] In many molecules, small basis sets usually overestimate the experimental covalent bond lengths. Therefore, it is often possible to find a basis set of intermediate quality which gives a geometry very close to the experiment. At this level of theory, the results are better than those obtained with much higher levels of theories; this is due to the opposing nature of correlation effects and basis set corrections, which tend to increase and decrease bonded distances, respectively.

On the basis of the aforementioned observations, computations at the HF level using valence double-zeta basis sets have long been used to predict geometries of molecules. However, it is difficult to predict *a priori* which basis set is optimal for a given molecule. Instead we must rely on experience gained in studies of similar molecules. The only reliable way to obtain molecular structures which converge toward the correct results is to use increasingly larger basis sets [e.g., 3-21G, 3-21G(d), 6-31G(d), double-zeta plus polarization, triple-zeta plus double polarization, etc.] and more complete treatment of electron correlation. Given the size of the molecules in the present study, only limited basis set dependence of the HF equilibrium molecular geometry can be studied. Inclusion of the correlation effects is prohibitively expensive for these molecules at a higher level than MP2. The GGA-DFT methods may provide a more economical alternative.

Table I shows that the HF method does not provide consistent results for Si—N distances in silatranes. The HF/3-21G calculations yielded a strongly polar Si—N bond for halogenosilatranes and fairly large differences between the Si—N distances depending on the substituent. In HF/3-21G(d) calculations, the d functions decrease the ionic character of the Si—N bonds and the dipole

moment of the molecules.[4] The HF/3-21G(*d*), 6-31G(*d*), and CEP-31G(*d*) results are similar to each other. The HF/CEP-31G(*d*) and HF/6-31G(*d*) results predict longer Si—N distances for 1-chlorosilatrane compared to 1-fluorosilatrane, while HF/3-21G and 3-21G(*d*) results predict the opposite (Table I).

The MP2 results shown in Table I clearly show that inclusion of the electron correlation is important to predict a reasonable Si—N distance. Given the importance of the correlation effects and the high cost of the MP2 calculations, we applied a more economical method to include electron correlation. The two selected GGA-DFT methods—namely, B3-P and B-P, yielded surprisingly consistent results (Table I). First we optimized the molecular geometries with normal grid and then we repeated the geometry optimizations with a fine grid. The grid size influences only slightly the Si—N distance, and the other bond lengths remain practically unchanged. The total energy increases slightly (by ~ 0.0001 Hartree). The GGA-DFT calculations provide shorter Si—N distances for 1-chlorosilatrane than for 1-fluorosilatrane (Table I).

Figures 1 and 2 show the fundamental differences between the HF/6-31G(*d*) and the B-P/6-31G(*d*5) equilibrium geometries for 1-chlorosilatrane. While the HF method provides too long an Si—N distance in equilibrium, the DFT methods provide a reasonable prediction for the gas phase structure of 1-chlorosilatrane in this respect.

There is considerable accumulated experience related to the reliability of the HF methods in predicting equilibrium geometries.[27] This is not true for the DFT methods, so analysis of the HF results can help check the DFT results and lead to reliable predictions.

Earlier studies of the basis set dependence of the Si—Cl single bond length in chlorosilane provided the following relations: r(3-21G) > r(6-31G(*d*)) > r(3-21G(*d*)) > r(experiment, ED).[27] The present study for 1-chlorosilatrane provides the same order (Table I). The HF/3-21G(*d*) and 6-31G(*d*) Si—Cl bond distances for 1-chlorosilatrane are 1 pm shorter than for chlorosilane. The B-P/6-31G(*d*5) method predicts the opposite: The Si—Cl bond length is longer in 1-chlorosilatrane than in chlorosilane (208.4 pm). This puts our estimate for the equilibrium (r_e) Si—Cl bond length around 206 pm in gas phase. The solid phase Si—Cl distance should be considerably longer because of the short Si—N distance and the medium effects (see discussion of Table II later in this article).

A basis set dependence study of the Si—O bond length in silanol provided the following order: r(3-21G) > r(experiment, ED) > r(6-31G(*d*)) > r(3-21G(*d*)).[27] The present study yielded the same order for silatranes (Table I). On the basis of HF results, the most probable gas phase Si—O distance in 1-chlorosilatrane can be between 166.0 and 164.5 pm [calculated at the 230 pm Si—N distance with 3-21G and 6-31G(*d*) basis sets, respectively]. We can also consider that the theoretical estimations for the Si—O bond lengths in 1-fluoro- and 1-chlorosilatrane are nearly equal to each other. Consequently, the Si—O bond length measured by ED in 1-fluorosilatrane (165.2 ± 0.3 pm) should not be far from the probable Si—O bond length in 1-chlorosilatrane. This value fits between the aforementioned lower and upper limits.

As it was mentioned earlier, at shorter Si—N distances the Si—O bond lengths are longer. However, the experimental results for the 1-fluorosilatrane seem to contradict to this prediction because the measured Si—O bond lengths are longer in the gas phase than in the solid phase (Table I). The explanation for this virtual Si—O bond shortening can be the shifting of the electron density on the oxygen atom toward the electron-deficient silicon atom because of the strongly electron-withdrawing fluorine in the neighborhood. This effect may overcompensate for the bond lengthening and result in a shorter X-ray Si—O bond length than expected. In 1-methylsilatrane this effect is obviously absent. For this molecule the X-ray experiment provides longer Si—O bond lengths than the ED experiment.

The basis set dependence of C—N, C—C, and C—O bond lengths illustrates well the results of the improper treatment of electron correlation at the HF level. The poorer basis sets provide better agreement with the experiment, and the relatively good quality 6-31G(*d*) basis set provides systematically too short bond lengths. Inclusion of the electron correlation (MP2 or DFT) lengthens these bonds, and the results agree well with the experiment. Earlier study of the basis set dependence of the C—N single bond length in methylamine provided the following order at the HF level: r(3-21G) = r(experiment, ED) > r(6-31G(*d*)).[27] The present study yielded a similar order for the C—N and C—C bond lengths in silatranes (Table I). The calculations with different substituents predict that the C—N bond length depends mostly on the Si—N distance (Fig. 3). The C—C bond lengths in silatranes agree well with the standard C—C bond length (154 pm), and this geometrical parameter

does not depend on the Si—N distance (Fig. 3). The predicted r_e structure agrees with the structure in Figure 2 except for the Si—N, Si—O, and Si—Cl distances, for which the corrected estimates are 230, 166, and 206 pm, respectively.

The calculated *ab initio* equilibrium C—H bond lengths are between 108.0 and 108.8 pm, depending on the position of the hydrogen atoms.

Dipole Moments and Self-Consistent Reaction Field Results

The calculated dipole moment is 8.662 Debye for 1-chlorosilatrane at the B-P/6-31G(*d*) level of theory. The dipole moment shows a nearly linear, slightly hyperbolic dependence of the Si—N distance. At shorter Si—N distances (below the equilibrium Si—N distance), the dipole moment increases more rapidly. To investigate the geometric effects of solvation, we apply the Onsager model.[28] This model uses a spherical cavity embedded in a continuum dielectric and a simple dipole-dipole interaction. It can be criticized because of the rough approximation of the cavity shape and neglect of the multipolar terms, which may play a role in the interaction. However, this model may reflect the basic medium effect. We compared the results for 1-fluorosilatrane and 1-chlorosilatrane. The molecular volume was defined as the volume inside a contour of 0.001 electrons/bohr^3 density, and the radius for use with the solvent reaction field was set to 50 pm larger than the radius corresponding to the computed volume (a procedure suggested in GAUSSIAN 92; the values are listed in Table II). The dielectric constant was set to 45 dimethylsulfoxide (DMSO). Because the optimized geometries change in the solvent field (Table II), we recalculated the cavity radius with the new equilibrium geometries and found no significant difference. The results in Table II show that 1-chlorosilatrane is more polarizable than 1-fluorosilatrane. The Si—N distance shortening, the Si—R bond lengthening, and the increase of the dipole moment are more pronounced in 1-chlorosilatrane than in 1-fluorosilatrane upon solvation. These results support the short Si—N and the long Si—Cl distances for 1-chlorosilatrane and they explain the surprisingly long Si—Cl distance in the solid phase experiment (chlorine is a better leaving group than fluorine). They also support a general Si—N distance shortening trend for silatranes during the transition from gas phase to polar liquid or solid phase. Table II also shows that the results are sensitive to the cavity size, and the smaller cavity leads to larger solvation effects. Our results are in qualitative agreement with the earlier semiempirical results[12] and with the HF self-consistent reaction field (SCRF) results of Gordon et al.[29]

The Correlated Potential Energy Curve for the Si—N Distance

It is known from previous studies[1-4] that the semiempirical and molecular mechanics (MM) methods predict the existence of the so-called exo form at large Si—N distances (above 300 pm). The

TABLE II.
B-P / 6-31G(*d*5) SCRF Results for 1-Chloro- and 1-Fluorosilatrane.[a]

	Cl	Cl	Cl	F	F
Cavity radius		**466** [b]	453		**453** [b]
dielectric constant	0.0	45.0	45.0	0.0	45.0
Energy	−1266.15140	−1266.14769	−1266.14681	−905.78060	−905.77849
Pol. energy	0.00000	−0.01480	−0.01702	0.00000	−0.01059
Dipole	8.662	11.617	11.947	7.496	9.422
r(Si—N)	228.6	217.8	216.9	230.2	221.4
r(Si—*X*)	210.1	214.7	215.3	162.3	163.6
r(Si—O)	169.3	169.5	169.5	169.1	169.6
r(N—C)	147.8	148.6	148.7	147.7	148.3
r(C—C)	153.8	153.7	153.7	154.0	153.9
r(O—C)	142.1	142.6	142.7	141.7	142.0

[a] The cavity radius and the bond lengths are in pm, the energies are in Hartree, the dipole moments are in Debye. The calculations were performed with a fine grid.
[b] Calculated equilibrium cavity radius.

HF results contradict these results. However, it is advisable to check the HF results with electron correlation methods. The MP2/CEP-31G(*d*) potential energy curve (PEC) calculations are too expensive. Therefore, we performed a series of MP2//PM3, MP2//HF, and a few MP2//MP2 calculations with the CEP-31G(*d*) basis set for 1-fluorosilatrane. The MP2//PM3 and MP2//HF notations stand for single-point MP2 calculation with the PM3 and HF geometry, respectively. The PM3 PEC shows a second minimum above the 310 pm Si—N distance. The MP2//PM3 PEC shows no minimum but a spurious shoulder above the 280 pm Si—N distance, which is absent on the MP2//HF curve. Near the minimum the MP2, HF, and PM3 curves are parallel, which signals a qualitative agreement between the three methods. However, at larger Si—N distances this agreement disappears. This behavior questions the reliability of the PM3 results and the existence of the exo minimum.

We calculated two relaxed points with the B-P/6-31G(*d*5) method at fixed 290 and 300 pm Si—N distances for 1-fluorosilatrane. The energy rises from −905.7748 to −905.7735 Hartree, and the negative gradient for the Si—N distance changes from −0.0065 to −0.0076 Hartree/Bohr. In an unconstrained molecular geometry optimization started with the 290 pm Si—N distance, the molecular geometry converged toward the endo equilibrium geometry. These results also predict that the exo form is nonexistent, in agreement with the HF results.[4,29]

Frequency Analysis

We checked the calculated minima by frequency analysis. It is not expected that the HF results provide wave numbers close to the experimental ones because of the known problems with HF frequencies and the rather poor equilibrium Si—N distances. Therefore, we performed a DFT frequency analysis for the 1-chloro-, 1-fluoro-, 1-methyl-, and 1-hydrogensilatrane at B-P/6-31G(*d*5) and B3-P/6-31G(*d*5) levels of theory with normal and fine grids. The total energies and the DFT zero point energies (ZPE) for various silatranes are listed in Table III. The wave numbers calculated at the B3-P/6-31G(*d*5) level of theory are systematically larger than the B-P/6-31G(*d*5) wave numbers. The latter are closer to the available experimental results. For example, the calculated B-P/6-31G(*d*5) CH_2 stretching wave numbers are in the range of 2920 to 3038 cm^{-1}, which is in good agreement with experimental results.[6] The B3-P/6-31G(*d*5) results provide larger wave numbers (by 100 cm^{-1}) and larger ZPE than the B-P/6-31G(*d*5) method (Table III). The performance of the normal grid was found to be satisfactory for silatrane molecules. The largest difference between the normal and fine grid results was 13 cm^{-1}, and the average of the differences was 0.4 cm^{-1}. The calculated results show that most of the silatrane skeleton vibrations show moderate dependence on the substituent, except for some silatrane breathing wave numbers. The Si—H stretching vibration is strong in 1-

TABLE III.
Total Energies (*E*) and Zero Point Energies (ZPE) for 1-Chloro-, 1-Fluoro-, 1-Methyl-, and Hydrogenosilatrane.[a]

	Cl		F		Me		H	
Method	*E*	ZPE	*E*	ZPE	*E*	ZPE	*E*	ZPE
HF / CEP-31G(*d*)	−115.28517		−124.47994				−101.11470	
MP2 / CEP-31G(*d*)	−116.85858		−126.07492				−102.55949	
HF / 3-21G(*d*)	−1255.53171		−897.06430					
HF / 6-31G(*d*)	−1261.80547		−901.78170		−841.89303		−802.84233	
MP2 / 6-31G(*d*)							−804.39901	
B-P / 6-31G(*d*5)	−1266.15146	0.1902	−905.78072	0.1916	−845.79619	0.2247	−806.47164	0.1971
B-P / 6-31G(*d*5)[b]	−1266.15140		−905.78060				−806.47150	
B3-P / 6-31G(*d*5)	−1268.13739		−907.62930	0.1987	−847.65499		−808.17968	
B3-P / 6-31G(*d*5)[b]			−907.62917	0.1986				

[a]The energies are in Hartrees.
[b]Calculated with a fine grid.

hydrogenosilatrane at 2236 cm^{-1}. The Si—F stretching wave number can be identified easily at 895 cm^{-1} in 1-fluorosilatrane; however, no pure Si—Cl vibration was found in the spectrum of 1-chlorosilatrane. The Si—Cl stretching is strongly coupled with the Si—N stretching, providing a peak at 513 cm^{-1}. The vibrational analysis also shows that the O—Si—N—C symmetric torsion is strongly coupled with the Si—N stretching at about 75 cm^{-1}, which is the lowest wave number in the spectra. We plan to model the medium effects for the infrared (IR) spectra of silatranes in the future. The complete list of the IR harmonic wave numbers and the normal coordinates is available on request from the authors.

Conclusions

The experimental structural parameters frequently contradict each other and the theoretical predictions for silatranes. The probable origin of these contradictions is the large-amplitude low-energy movements of the carbon atoms of the ethoxy links and the presence of the two enantiomer structures. With the help of semiempirical, *ab initio*, and DFT calculations, the uncertain geometrical parameters of the experimental results can be discovered. For example, the calculations do not support the short C—C and C—N bond lengths, the large C—C—N bond angle, and the flat ring structures found in the X-ray experiment for 1-chlorosilatrane.

To predict reliable theoretical Si—N distances for the gas phase structures, the electron correlation should be included. In this respect the GGA-DFT calculations provide good results with a moderate size [6-31G(*d*5)] basis set. The Si—N distance can be reliably calculated with the normal pruned grid of GAUSSIAN 92. The fine pruned grid provides only a slight change (2–3 pm) in this respect. The B-P/6-31G(*d*5) calculations provide 233 and 245 pm for the gas phase Si—N equilibrium distance in 1-fluoro- and 1-methylsilatrane, respectively, which are in excellent agreement with the ED results. However, the calculations do not support the large (116°) O—C—C bond angles and the C—O—Si—N and O—Si—N—C dihedral angles found in the ED experiment. We have found that the transition between the $\mathbf{OC}_0$ and the $\mathbf{CN}_0$ envelope conformations of the anellated five-membered rings consists of a series of twisted conformations and that during this transition the Si—N distance gradually decreases; the bond lengths and bond and dihedral angles of the rings change, except for the C—C and C—O bond lengths. The $\mathbf{OC}_0$ and the $\mathbf{CN}_0$ envelopes are reproduced by the HF/3-21G(*d*) equilibrium geometries at 260 and 200 pm Si—N distances, respectively. The HF results provide that 1 kcal/mol energy is sufficient to change the Si—N distance by ±25 pm. This flexibility leads to large changes in the Si—N distance and in the ring conformations as the medium changes. The X-ray geometry of 1-fluorosilatrane with a 204 pm Si—N distance corresponds to the $\mathbf{CN}_0$ envelope conformation, which supports the theoretical prediction.

The SCRF GGA-DFT results show that the Si—N distance shortening, the Si—R bond lengthening, and the increase of the dipole moment are more pronounced in 1-chlorosilatrane than in 1-fluorosilatrane upon solvation (chlorine is a better leaving group than the fluorine). These results support the short Si—N and the long Si—Cl distances for 1-chlorosilatrane, and they explain the surprisingly long Si—Cl distance in the X-ray experiment. They also support a general Si—N distance shortening trend for silatranes during the transition from gas phase to polar liquid or solid phase.

The exo form predicted by the semiempirical methods is not supported by any of the higher-level methods. The frequency analysis of silatranes shows a number of low-energy vibrations. The symmetric O—Si—N—C torsion is the lowest-energy vibration at about 75 cm^{-1}. The Si—H and Si—F stretching wave numbers are easily identifiable at 2236 cm^{-1} and at 895 cm^{-1}, respectively. The Si—Cl stretching vibration is coupled with the Si—N stretching.

Acknowledgments

The authors are indebted to Professor Mark S. Gordon and Dr. Michael W. Schmidt for their submitted manuscript and for their comments. The financial support of the Hungarian Research Foundation (OTKA Nos. T644, T4098, and T14247) is acknowledged.

References

1. G. I. Csonka and P. Hencsei, *J. Organomet. Chem.*, **446**, 99 (1993).

2. G. I. Csonka and P. Hencsei, *J. Mol. Struct. (Theochem)*, **283**, 251 (1993).
3. G. I. Csonka and P. Hencsei, *J. Organomet. Chem.*, **454**, 15 (1993).
4. G. I. Csonka and P. Hencsei, *J. Comput. Chem.*, **15**, 385 (1994).
5. P. Hencsei, *Struct. Chem.*, **2**, 21 (1991), and references cited therein.
6. L. Párkányi, P. Hencsei, L. Bihátsi, and T. Müller, *J. Organomet. Chem.*, **269**, 1 (1984).
7. G. Forgács, M. Kolonits, and I. Hargittai, *Struct. Chem.*, **1**, 245 (1990).
8. L. Párkányi, L. Bihátsi, and P. Hencsei, *Cryst. Struct. Commun.*, **7**, 435 (1978).
9. Q. Shen and R. L. Hilderbrandt, *J. Mol. Struct.*, **64**, 257 (1980).
10. A. A. Kemme, Ya. Ya. Bleidelis, V. A. Pestunovich, V. P. Baryshok, and M. G. Voronkov, *Dokl. Akad. Nauk SSSR*, **243**, 688 (1978).
11. C. Glidewell, *Inorg. Chim. Acta*, **20**, 113 (1976).
12. V. F. Sidorkin, G. K. Balakchi, M. G. Voronkov, and V. A. Pestunovich, *Dokl. Akad. Nauk SSSR*, **301**, 1235 (1988).
13. R. Krishnan, M. J. Frisch, and J. A. Pople, *J. Chem. Phys.*, **72**, 4244 (1980) and references cited therein.
14. A. D. Becke, *Phys. Rev. A*, **38**, 3098 (1988).
15. J. P. Perdew, *Phys. Rev. B*, **33**, 8822 (1986).
16. S. H. Vosko, L. Wilk, and M. Nussair, *Can. J. Phys.*, **58**, 1200 (1980).
17. A. D. Becke, *J. Chem. Phys.*, **98**, 5648 (1993).
18. M. J. Frisch, G. W. Trucks, M. Head-Gordon, P. M. W. Gill, M. W. Wong, J. B. Foresman, B. G. Johnson, H. B. Schlegel, M. A. Robb, E. S. Replogle, R. Gomperts, J. L. Andres, K. Raghavachari, J. S. Binkley, C. Gonzalez, R. L. Martin, D. J. Fox, D. J. DeFrees, J. Baker, J. J. P. Stewart, and J. A. Pople, Gaussian 92/DFT, Revision G, Gaussian, Inc., Pittsburgh PA, 1993.
19. W. J. Stevens, H. Basch, and M. Krauss, *J. Chem. Phys.*, **81**, 6026 (1984).
20. (a) W. J. Hehre, R. Ditchfield, and J. A. Pople, *J. Chem. Phys.*, **56**, 2257 (1972); (b) M. M. Francl, W. J. Pietro, W. J. Hehre, J. S. Binkley, M. S. Gordon, D. J. DeFrees, and J. A. Pople, *J. Chem. Phys.*, **77**, 3654 (1982); (c) W. J. Pietro, M. M. Francl, W. J. Hehre, D. J. DeFrees, J. A. Pople, and J. S. Binkley, *J. Am. Chem. Soc.*, **104**, 5039 (1982).
21. (a) J. W. Turley and F. P. Boer, *J. Am. Chem. Soc.*, **90**, 4026 (1968); (b) L. Párkányi, J. Nagy, and K. Simon, *J. Organomet. Chem.*, **101**, 10 (1975); (c) L. Párkányi, K. Simon, and J. Nagy, *Acta Cryst. Sect. B.*, **30**, 2328 (1974).
22. A. A. Kemme, Thesis, Riga, 1977.
23. A. A. Kemme, Ya. Ya. Bleidelis, V. M. Dyakov, and M. G. Voronkov, *Zhurn. Struct. Khim.*, **16**, 914 (1975).
24. Ya. Ya. Bleidelis, *PSR Zinat. Akad. Vestis, Khim. Ser.*, 1983, p. 259.
25. V. Fülöp, A. Kálmán, P. Hencsei, G. Csonka, and I. Kovács, *Acta. Cryst. C*, **44**, 720 (1988).
26. L. Párkányi, P. Hencsei, G. Csonka, and I. Kovács, *J. Organomet. Chem.*, **329**, 305 (1987).
27. W. J. Hehre, L. Radom, P. v. R. Schleyer, and J. A. Pople, *Ab Initio Molecular Orbital Theory*, John Wiley & Sons, New York, 1986.
28. M. W. Wong, K. B. Wiberg, and M. J. Frisch, *J. Am. Chem. Soc.*, **114**, 1645 (1992) and references cited therein.
29. M. W. Schmidt, T. L. Windus, and M. S. Gordon, *J. Am. Chem. Soc.*, **117**, 7480 (1995).